# Impurity nearest-neighbor distances studied by extended x-ray absorption fine structure: Application to electron-spin resonance

J. Azoulay and E. A. Stern
*Department of Physics, FM-15, University of Washington, Seattle, Washington 98195*

D. Shaltiel and A. Grayevski
*Racah Institute of Physics, The Hebrew University of Jerusalem, Jerusalem, Israel*
(Received 21 December 1981)

The local environment around Pr as a magnetic impurity in ErSb solid solutions was investigated by extended x-ray absorption fine structure measurements on $Er_xPr_{1-x}Sb$ ($x=1, 0.95, 0.90$). The nearest-neighbor distances around the Pr ion were found to be nearly the same as in pure PrSb, almost independent of the Pr concentration in the alloys. Thus, the usual assumption used in electron-spin-resonance measurements—that the impurity nearest-neighbor distance is the same as that of the host—is incorrect.

## I. INTRODUCTION

It has long been recognized theoretically[1] that the crystal electric field (CEF) parameters $b_n$ are strongly influenced by the local environment of the magnetic ion. Using the point charge (PC) model, Lea *et al.*[1] established an inverse fifth-power relation between $b_4$ and the nearest-neighbor distances and an inverse seventh-power relation for $b_6$. In many cases a magnetic impurity ion is inserted in the host material to probe the local environment. In such a case an assumption has to be made about the value of the nearest-neighbor distance since the impurity will, in general, disturb the lattice. The usual assumption is to neglect this disturbance and assume the host nearest-neighbor distance, which is proportional to the lattice constant $a_0$.

From the data analysis of his ESR measurments on $Dy^{2+}$ impurities in the cubic insulators $CaF_2$, $SrF_2$, and $BaF_2$, Kiss[2] was able to show that $b_4$ varies more like $a^{-2}$ than like $a_0^{-5}$. Deviation from the PC model in some cubic metallic compounds was also reported by Davidov *et al.*[3,4] Surprisingly, in spite of the disagreement, the basic assumption of neglecting the disturbance of the impurities is rarely questioned. As far as we are aware, there exists so far no research work in which possible lattice deformations of the host crystal by the impurity probes were measured and considered. Therefore it is of fundamental importance for ESR spectra interpretation to investigate this question.

To obtain information on the impurity ion's local vicinity we have used extended x-ray absorption fine structure (EXAFS) spectroscopy. EXAFS is observed in the form of fine structure that appears on the high-energy side of the x-ray absorption edge for transitions from the $K$ or $L$ shells.[5–7] Generally extending from 40 eV to more than 1000 eV past the edge, this fine structure is created by a modulation of the absorption matrix element which is caused by interference between the outgoing spherical wave of the photoelectron and waves backscattered from the neighboring atoms. As the x-ray energy is changed, the interference varies between constructive and destructive, giving rise to the modulation in the x-ray absorption coefficient as a function of energy. These modulations can be analyzed to obtain the atomic arrangement of the nearby environment of the excited central atom.

The basic equation describing the EXAFS spectrum at the $K$ shell in the one-electron picture is given by[8,9]

$$\chi(k)=\sum_i \frac{N_i f_i(k)}{kR_i^2}\exp\left[-2k^2\sigma_i^2-\frac{2R_i}{\lambda}\right] \times \sin[2kR_i+\delta_i(k)] \ . \quad (1)$$

The equation is also valid for the $L$ shell to a good approximation for cubic environments.[10,11] The photoelectron wave number $k$ is related to its energy $E$ by $\hbar^2k^2/2m=E-E_0$, where $E_0$ and $m$ are the binding energy and mass of the electron. The sum is over coordination shells at distances $R_i$, each of which contains $N_i$ similar atoms at the average distance $R_i$ from the center atom. The Debye-Waller-type factor $\exp(-2k^2\sigma_i^2)$ takes account of thermal motion and/or structural disorder in a given coordination shell, and $\lambda$ is a mean free path which accounts for the finite lifetime of the excited state consisting of the photoelectron and the ionized atom. The functions $f_i(k)$ and $\delta_i(k)$ are, respectively, the backscattering amplitude and the total phase shift introduced by the atomic potentials.

 

In this paper we present a detailed study of the Pr-Sb interatomic distance in three different ErPrSb solid solutions which reveals a considerable lattice distortion of the host in the vicinity of the Pr ion.

## II. EXPERIMENT

We have measured the EXAFS spectrum of $Er_xPr_{1-x}Sb$, where $x=1$, 0.95, and 0.90 on the $L_{III}$ edge of Er. The samples were prepared in an argon-arc furnace from stoichiometric amounts of high-purity Er, Pr, and Sb. A subsequent x-ray analysis indicated less than 2% oxidation. The samples were then ground to a fine powder, sieved through 400 mesh, and spread uniformly onto 0.05-mm-thick magic transparent Scotch tape. Eight layers of tape, used to make the sample with measured thickness around the theoretical optimum to minimize thickness effects,[12] were placed in copper cells with Kapton x-ray windows sealed with epoxy. The cells were sealed with indium O rings after the sample was placed inside.

All the EXAFS spectrum measurements were acquired at the Stanford Synchrotron Radiation Laboratory (SSRL) using beam line IV-3 (wiggler line) at room temperature only. In order to estimate the error bar, each sample was subjected to at least three different scans, each of which had a total of $10^9$ photons per data point. A typical spectrum is presented in Fig. 1.

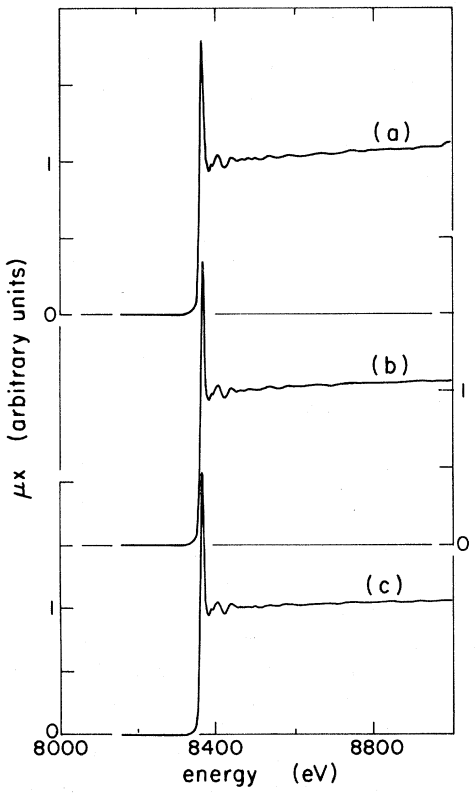


FIG. 1. The $L_{III}$ edge x-ray absorption spectrum of Er as a function of the x-ray photon energy in (a) ErSb, (b) $Er_{0.95}Pr_{0.05}Sb$, (c) $Er_{0.90}Pr_{0.10}Sb$, after pre-edge background subtraction and normalization to the edge step.

A silicon (220) crystal monochromator was used in all cases. The incident and final x-ray intensities were measured using ionization chambers filled with appropriate gases. The monochromator was routinely detuned to reduce contamination from harmonics, which were monitored on a rate meter connected to the output of a photomultiplier placed behind the second ionization chamber and shielded by 9.4-mm aluminum. The overall energy resolution in the absorption measurements was better than 1 eV in all cases.

## III. DATA ANALYSIS

The $L_{III}$ edge of Er was isolated from the rest of the absorption spectra by removing a smooth pre-edge fitted curve. The data were then normalized and interpolated from energy to $k$ space using $k=[2m(E-E_0)]^{1/2}/\hbar$, where $E_0$ was set to the peak of the "white line" at the top of the edge. A second smooth curve was then subtracted to remove the smooth $\mu_0$ contribution from the data, thus leaving a pure EXAFS oscillatory signal. The low-$k$ value limit of 4.2 $Å^{-1}$ for the $\chi(k)$ data analysis was set by the requirement of being beyond the white line of Fig. 1 (the large peak near the edge), while the upper limit was chosen to be $k=10.7$ $Å^{-1}$, above which the signal-to-noise ratio became too small to be useful.

A single coordination shell was then isolated by Fourier transform of $k^2\chi(k)$ with respect to $\exp[-i(2kr)]$, yielding peaks corresponding to the neighboring shells of atoms.[8] To simplify the analysis, the EXAFS contribution from individual shells was isolated by back Fourier filtering using a suitable $\vec{r}$-space window with a Hanning function to provide a smooth termination of the window. We applied a 2.00–3.50-Å $\vec{r}$-space window along with a Hanning function width of 0.1 Å at both ends of the window (Fig. 2). The backtransform can be analyzed[11] to obtain separately the total phase of the sine function and its coefficient in (1)—the amplitude—as functions of $k$. Using ErSb compound as a standard, the difference in phases between ErSb and each of the compounds $Er_xPr_{1-x}Ab$ ($x=0.95$, 0.90) was calculated.[11] Since the backscattering atoms are of the same type in both, the phase difference is $2k(R_2-R_1)$, where $R_2$ and $R_1$ are the distances to the neighboring coordination shells in the sample and the standard, respectively. A plot of the phase difference versus $k$ yields[7,11] a straight line of slope $2(R_2-R_1)$. Similarly, by plotting the logarithm of

TABLE I. EXAFS and x-ray diffraction results for ErPrSb alloys. Results in columns a and b are obtained from EXAFS measurements using ErSb as the standard. Values in column c are obtained from x-ray diffraction measurements. Pr-Sb interatomic distances in column d are calculated from results in columns b and c. Values in column e are obtained by using results from column d and those from Ref. 15.

| Sample | a $\ln\frac{N_1R_2^2}{N_2R_1^2}$ | b $R$(Er-Sb) (Å) | c $a_0/2$ (Å) | d $R$(Pr-Sb) (Å) | e CEF (MeV) |
|---|---|---|---|---|---|
| ErSb | ... | ... | 3.054 ±0.001 | ... | ... |
| $Er_{0.95}Pr_{0.05}Sb$ | −0.128 | 3.054 ±0.007 | 3.063 ±0.002 | 3.2 ±0.1 | 7.8 |
| $Er_{0.90}Pr_{0.10}Sb$ | −0.062 | 3.054 ±0.007 | 3.071 ±0.001 | 3.22 ±0.04 | 8.0 |
| PrSb | ... | ... | 3.185 | 3.185 | 8.5 |

the ratio of the amplitudes versus $k^2$ a straight line of slope equal to twice the difference between $\sigma^2$ and the intercept of $\ln(N_1R_2^2/N_2R_1^2)$ at $k=0$ is obtained.[7,11]

The final results are summarized in Table I. The results shown in columns a and b were obtained from the EXAFS measurements by using ErSb as the standard. The lattice constants in column c were obtained from x-ray diffraction measurements. The values of $R$(Pr-Sb)—the Pr-Sb interatomic distance—in column d were obtained by using the relation

$$R(\mathrm{Er}_x\mathrm{Pr}_{1-x}\mathrm{Sb}) = xR(\text{Er-Sb}) + (1-x)R(\text{Pr-Sb}) \ ,$$

where $R(\mathrm{Er}_x\mathrm{Pr}_{1-x}\mathrm{Sb})$ is the mean interatomic distance in the solid solution $\mathrm{Er}_x\mathrm{Pr}_{1-x}\mathrm{Sb}$ as measured by x-ray diffraction and $R$(Er-Sb) is the Er-Sb interatomic distance as observed by EXAFS measurements on the $L_{\mathrm{III}}$Er edge in the same $\mathrm{Er}_x\mathrm{Pr}_{1-x}\mathrm{Sb}$ solid solution.

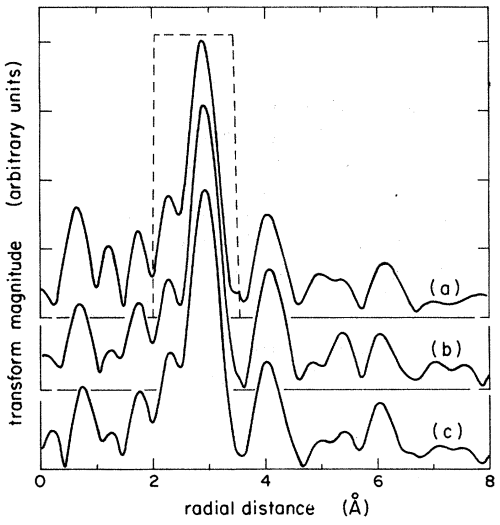


FIG. 2. The magnitude of the Fourier transform of $k^2\chi(k)$ over the range 4.2 Å$^{-1} \leq k \leq$ 10.7 Å$^{-1}$ plotted on the same scales for (a) ErSb, (b) $Er_{0.95}Pr_{0.05}Sb$, (c) $Er_{0.90}Pr_{0.10}Sb$. The dotted line in (a) indicates the windows in $\vec{r}$ space used to isolate and backtransform the first peak into $\vec{k}$ space.

## IV. DISCUSSION

According to the PC theory,[1] the fourth-order crystalline field parameter in a cubic crystal-field potential is predicted to follow a $Ze^2R^{-5}$ behavior, where $R$ is the distance of the coordinating charges $Ze$ from the magnetic ion, traditionally assumed to be the host-lattice constant. However, when using this approximation the value of $b_4$ for Gd in LaSb is expected to be larger than that in YSb, which is in conspicuous disagreement with the experiment.[3] Similar inconsistency has been reported for the pairs LaBi-YBi and LaAs-YAs by Urbant *et al.*,[13] who note a general tendency of increasing $b_4$ vs $a_0$.

Our EXAFS analysis together with the x-ray diffraction shows without any doubt that there is a considerable lattice distortion around the probe ion, as clearly demonstrated by Fig. 3 and Table I. In particular, the Er-Sb and Pr-Sb distances in the $x=0.90$ alloy are significantly different from the value deter-

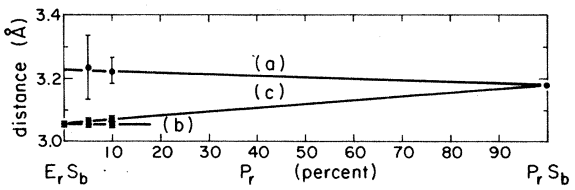


FIG. 3. Interactomic distances vs composition for (a) Pr-Sb, using results from Table I, and (b) Er-Sb, obtained from EXAFS results; (c) shows half-average lattice constant values determined by x-ray diffraction as a function of composition.

mined from the average lattice constant, i.e., $a_0/2$. Our results indicate that the Pr-Sb interatomic distance in $Er_xPr_{1-x}Sb$ compounds is nearly the same as in the pure Pr-Sb compound rather than the value calculated from ErSb lattice constants. This rules out any justification for the standard assumption. In view of the extreme sensitivity of the PC theory to the distance $R$, this distortion must be taken into account. In fact Kiss[2] has predicted a 7% contraction from the lattice constant of the cubic host $CaF_2$, $SrF_2$, and $BaF_2$ if the observed cubic crystal-field splitting were to be fitted to the $R^{-5}$ rule. The fact that the field resonance for both systems YSb:Er and LaSb:Er as observed by ESR measurements[3] are the same is consistent with our results.

The fact that the local neighborhood around the Pr impurity is approximately independent of the concentration of the impurity and is essentially the same as in pure PrSb is not an isolated result. This is a rather general phenomenon as exemplified by Vegard's law, which states

$$d_m = xd_B + (1-x)d_A \ , \tag{2}$$

where $d_m$ is the mean atomic distance in the solid solution composed of components $A$ and $B$, having interatomic distances $d_A$, and $d_B$, and $x$ is the fraction of $B$ atoms present in the solution. Experimentally, $d_B$ and $d_A$ are constants independent of $x$ for many classes of solid solutions.

The most powerful spectroscopic tool for determining the CEF parameter $b_4$ for rare-earth metallic compounds is the inelastice neutron scattering technique,[14,15] where the magnetic dipole transitions between the CEF levels are probed. The complications introduced by the lattice deformation in the presence of impurities was avoided by using this technique to measure the CEF parameters in the rare-earth monomphosphides $RP$($R$ =Ce, Pr, Nd, Sm, Tb, Ho, Er, Tm, Yb).[15] Using these results together with the Pr-Sb distances presented in Table I, the values of the fourth-order crystal-field parameter in the $Er_xPr_{1-x}Sb$ ($x$ =1, 0.95, 0.90) were predicted (Table I).

In conclusion, we have shown that the usual assumption in evaluating the nearest-neighbor distances around magnetic impurity probes, namely, that it is the same as in the host, is incorrect in the case of Pr impurities in ErSb. In fact we find that the Pr-Sb distance for the impurity is essentially the same as in pure PrSb. This result is as generally applicable as Vegard's law. In fact, a measurement of the mean lattice constant by x-ray diffraction as a function of composition can be used to determine the correct impurity nearest-neighbor distance. If Vegard's law is approximately satisfied, then the distance is approximately the same as in the pure material of the impurity obtained by extrapolating to 100% of the impurity.

## ACKNOWLEDGMENTS

This research was supported by NSF Grant No. DMR 80-22221. We are indebted to the staff of SSRL, whose facilities were supported by NSF Grant No. DMR 77-27487.

[1]M. R. Lea, M. J. M. Leask, and W. P. Wolf, J. Phys. Chem. Solids 23, 1381 (1962).
[2]Z. J. Kiss, Phys. Rev. 137A, 1749 (1965).
[3]D. Davidov, C. Rettori, and D. Shaltiel, Phys. Lett. 50A, 392 (1974).
[4]D. Davidov, C. Rettori, G. Ng, and E. P. Chock, Phys. Lett. 49, 320 (1974).
[5]E. A. Stern, Phys. Rev. B 10, 3027 (1974).
[6]F. W. Lytle, D. E. Sayers, and E. A. Stern, Phys. Rev. B 11, 4825 (1975).
[7]E. A. Stern, D. E. Sayers, and F. W. Lytle, Phys. Rev. B 11, 4836 (1975).
[8]E. A. Stern, Contemp. Phys. 19, 289 (1978).
[9]P. A. Lee and J. B. Pendry, Phys. Rev. B 11, 2795 (1975).
[10]F. W. Lytle, D. E. Sayers, and E. A. Stern, Phys. Rev. B 15, 2426 (1977).
[11]E. A. Stern and S. M. Heald (unpublished).
[12]E. A. Stern and K. Kim, Phys. Rev. B 23, 3781 (1981).
[13]P. Urban and D. Seipler, J. Phys. F 7, 1589 (1977).
[14]K. C. Turberfield, L. Passell, R. J. Birgeneau, and E. Bucher, Phys. Rev. Lett. 25, 752 (1970).
[15]R. J. Birgeneau, E. Bucher, J. P. Matia, L. Passell, and K. C. Turberfield, Phys. Rev. B 8, 5345 (1973).